Electronic supplementary information

Low-cost green synthesis of zinc sponge for rechargeable, sustainable batteries

Brandon J. Hopkins,*[a] Christopher N. Chervin,[b] Megan B. Sassin,[b] Jeffrey W. Long,[b] Debra R. Rolison,*[b] and Joseph F. Parker[b]

[a] Naval Research Laboratory–National Research Council Postdoctoral Associate
Email: brandon.hopkins.ctr@nrl.navy.mil
[b] Surface Chemistry Branch, U. S. Naval Research Laboratory, Code 6170, Washington, DC 20375, USA
Email: debra.rolison@nrl.navy.mil

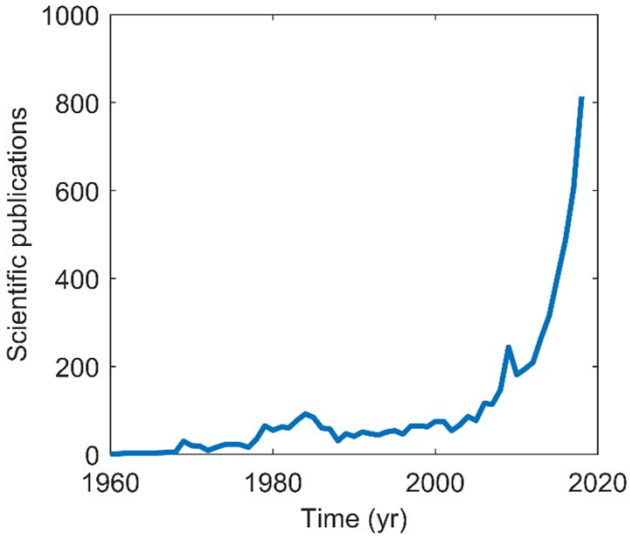

ESI Fig. 1 Growing interest in Zn batteries. Scientific publication count versus time. The data derive from Scopus, Elsevier's citation database, using the search term "zinc batteries."

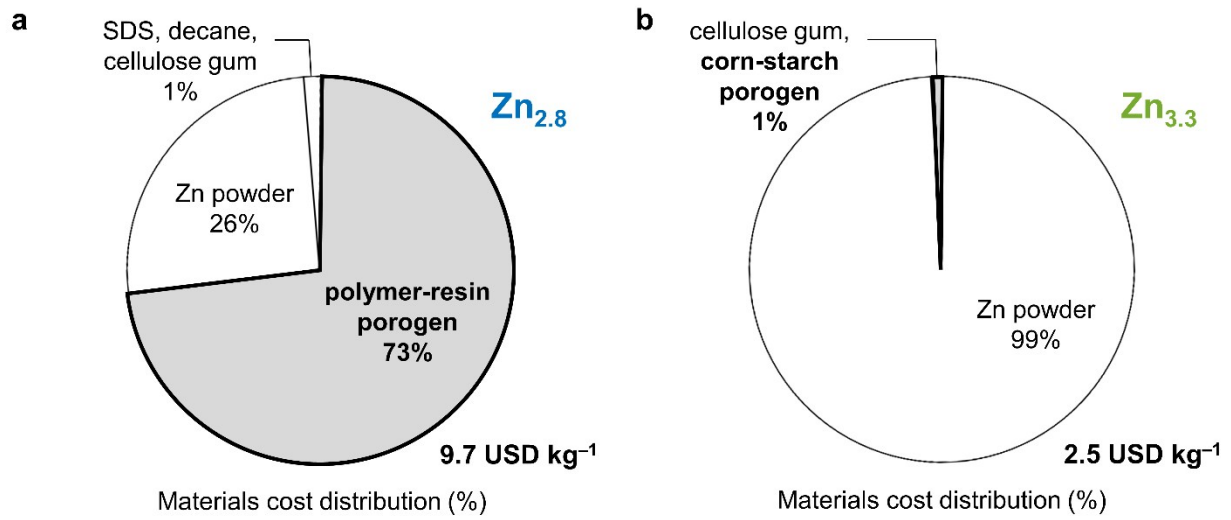

ESI Fig. 2 Materials cost distribution of $Zn_{2.8}$ and $Zn_{3.3}$ sponges. (a) Materials cost distribution of $Zn_{2.8}$. (b) Materials cost distribution of $Zn_{3.3}$. The sponges use the following ingredients: decane (2 USD kg^{-1}), polymer-resin porogen (CMC resin: 420 USD kg^{-1}), Zn (2.5 USD kg^{-1}), cellulose gum (1 USD kg^{-1}), sodium dodecyl sulfate or SDS (1.5 USD kg^{-1}), and corn starch (0.3 USD kg^{-1}).

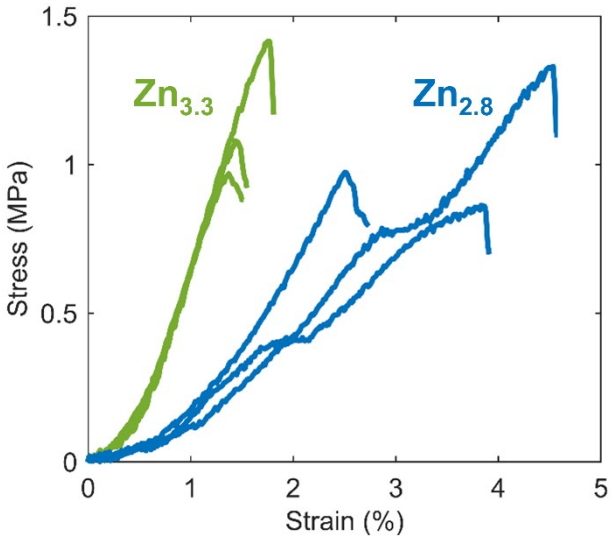

ESI Fig. 3 Tensile stress versus strain of $Zn_{2.8}$ and $Zn_{3.3}$ sponges. We measured tensile stress using diametral compression testing at a constant displacement rate of 1 mm min^{-1}. The diameter of the cylindrical samples were 11.5 mm with thickness of 4 mm. The $Zn_{2.8}$ and $Zn_{3.3}$ sponges yielded maximum tensile strengths of 1.1 ± 0.2 MPa and 1.2 ± 0.2 MPa, respectively. We calculated standard deviations based on the three trials shown for each sponge.

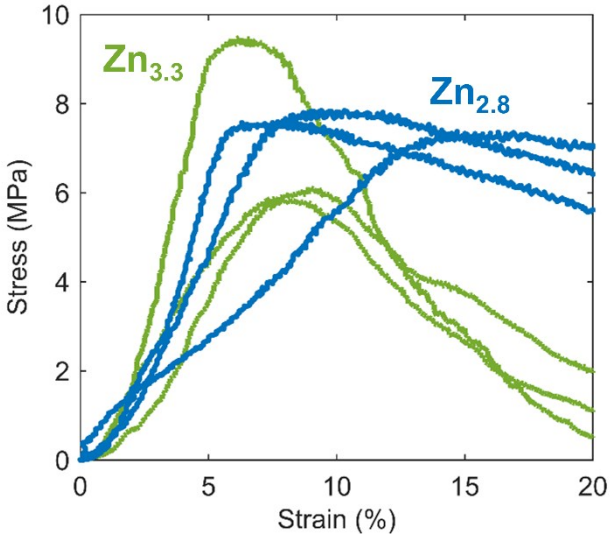

ESI Fig. 4 Compressive stress versus strain of $Zn_{2.8}$ and $Zn_{3.3}$ sponges. We measured compressive stress using uniaxial compression testing at a constant displacement rate of 1 mm min^{-1}. The diameter of the cylindrical samples were 11.5 mm with thickness of 4 mm. The $Zn_{2.8}$ and $Zn_{3.3}$ sponges yielded maximum tensile strengths of 7.6 ± 0.2 MPa and 7.1 ± 2.0 MPa, respectively. We calculated standard deviations based on the three trials shown for each sponge.

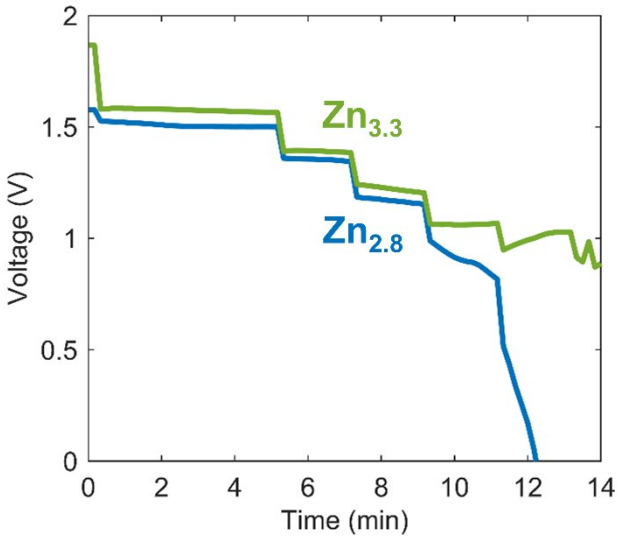

ESI Fig. 5 Voltage versus time of $Zn_{3.3}$ and $Zn_{2.8}$ electrodes in Ag–Zn cells. Both cells were discharged at 10 mA cm_{geo}^{-2} for 5 min as a break-in procedure. Thereafter they were discharged at 50, 100, 150, 200, and 250 mA cm_{geo}^{-2} for 2 min. The $Zn_{2.8}$ and $Zn_{3.3}$ sponges reach peak powers of 134 ± 8 mW cm_{geo}^{-2} and 199 ± 6 mW cm_{geo}^{-2}, respectively. Standard deviations were calculated based on the data collected for each time interval at a given current density.

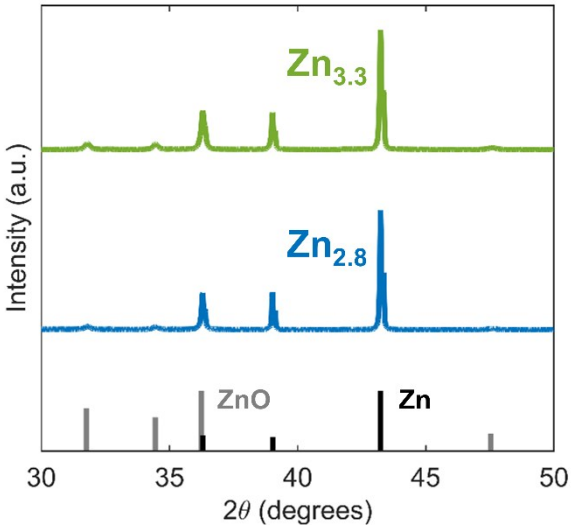

ESI Fig. 6 X-ray powder diffraction of $Zn_{2.8}$ and $Zn_{3.3}$. Based on relative intensities measured from ground-up Zn sponges indexed to Zn (ICDD #01-078-9363) and ZnO (ICDD #00-005-0664), the Zn content was 72 and 78% for $Zn_{2.8}$ and $Zn_{3.3}$, respectively, with ZnO as the remaining percentage.

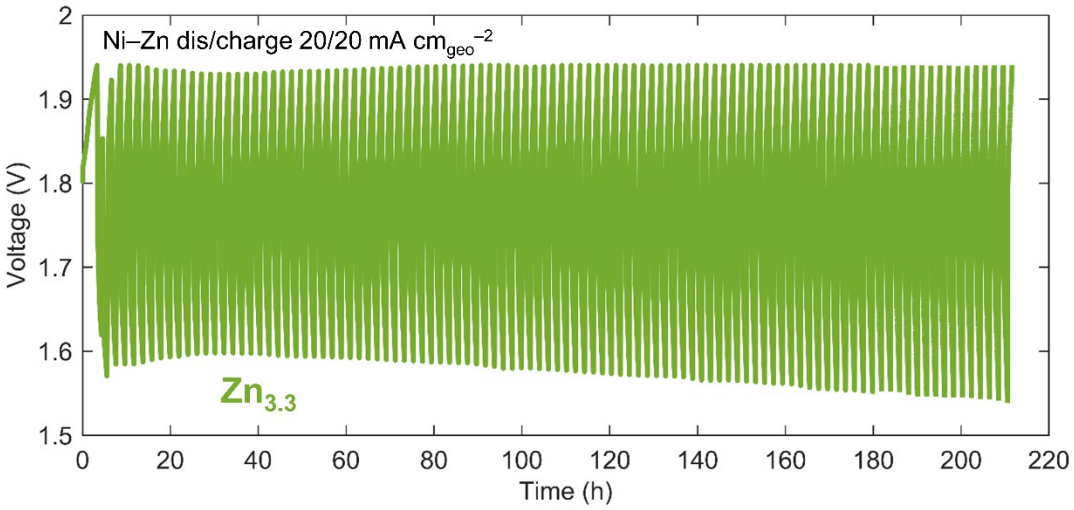

ESI Fig. 7 Voltage versus time of $Zn_{3.3}$ electrode cycled at 20 mA cm_{geo}^{-2} over 100 times in a Ni–Zn cell. The initial, irregular voltage profiles were due to a potentiostat programming error that was corrected for the remaining cycles. The cutoff voltages were 1.3 to 1.94 V. A coulombic efficiency of 99 to 100% was maintained with a rechargeable capacity of 20.5 mA h, corresponding to 10% DOD_{Zn}.

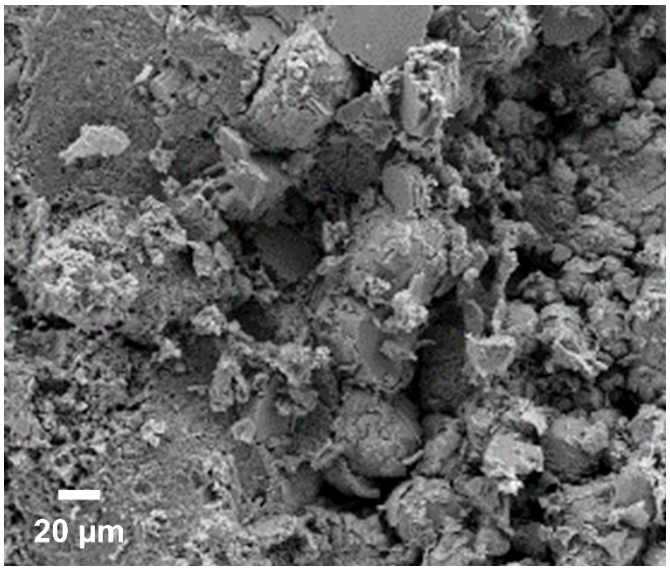

ESI Fig. 8 Microscopic analysis of post-cycled cross-sectioned $Zn_{3.3}$ from a Ni–Zn cell cycled at 20 mA cm_{geo}^{-2} over 100 times. Scanning electron micrograph of $Zn_{3.3}$ after cycling protocol shown in ESI Fig 7.

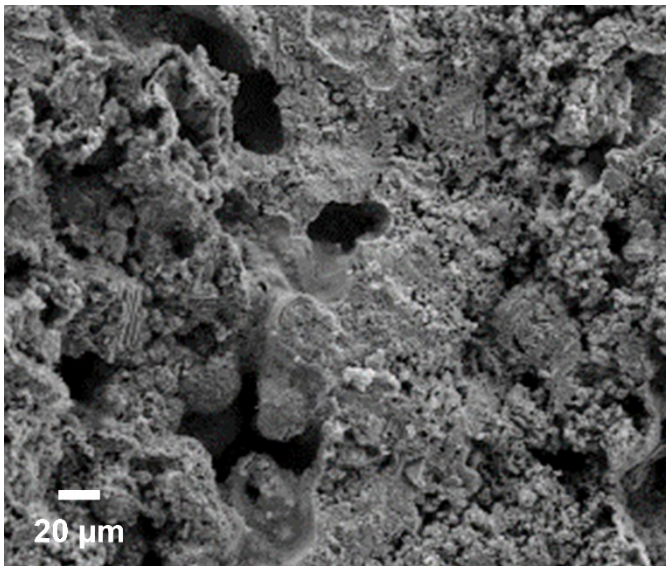

ESI Fig. 9 Microscopic analysis of post-cycled cross-sectioned $Zn_{3.3}$ from a Zn–air cell. Scanning electron micrograph of $Zn_{3.3}$ after cycling as shown in Fig. 4c.

ESI Table 1 European Union supply risk and the weight percentage of battery-relevant elements in the Earth's upper continental crust. Elements listed in bold are abundant and low risk.

Element	Abundance (wt%)	Supply risk
Iridium (Ir)	0.0000000022	2.5
Ruthenium (Ru)	0.000000034	2.5
Platinum (Pt)	0.00000005	2.5
Palladium (Pd)	0.000000052	2.5
Tellurium (Te)	0.0000001	0.8
Gold (Au)	0.00000015	0.2
Silver (Ag)	0.0000053	0.6
Indium (In)	0.0000056	2.4
Selenium (Se)	0.000009	0.4
Bismuth (Bi)	0.000016	3.8
Antimony (Sb)	0.00004	4.4
Tantalum (Ta)	0.00009	1.1
Molybdenum (Mo)	0.00011	0.9
Germanium (Ge)	0.00014	1.8
Tungsten (W)	0.00019	1.8
Tin (Sn)	0.00021	0.8
Beryllium (Be)	0.00021	2.5
Gadolinium (Gd)	0.0004	4.9
Samarium (Sm)	0.00047	5.0
Praseodymium (Pr)	0.00071	5.0
Niobium (Nb)	0.0012	3.2
Scandium (Sc)	0.0014	2.9
Lead (Pb)	0.0017	0.1
Cobalt (Co)	0.0017	1.5
Gallium (Ga)	0.0018	1.5
Lithium (Li)	0.0021	1.1
Yttrium (Y)	0.0021	4.9
Lanthanum (La)	0.0031	5.0
Cerium (Ce)	0.0063	5.0
Vanadium (V)	0.0097	1.5
Phosphorus (P)	0.066	4.1
Magnesium (Mg)	1.50	4.0
Silicon (Si)	31.14	1.1
Copper (Cu)	**0.0028**	**0.2**
Nickel (Ni)	**0.0047**	**0.4**
Zinc (Zn)	**0.0067**	**0.4**
Chromium (Cr)	**0.0092**	**0.9**
Sulfur (S)	**0.062**	**0.7**
Manganese (Mn)	**0.077**	**0.9**
Titanium (Ti)	**0.38**	**0.3**
Iron (Fe)	**3.92**	**0.8**
Aluminum (Al)	**9.67**	**0.5**

ESI Table 2 System cost and specific energy of batteries that rely on abundant, low-risk elements as defined by Fig. 1a. Batteries listed in bold are based on Zn. References are found in the main text.

System	Cost (USD kWh_{sys}^{-1})	Specific Energy (W h kg^{-1})	Reference†
Ni–Fe	70	40	11, 11
Zn–MnO_2	**90**	**75**	**12, 13**
Fe–air	100	60	14, 14
Zn–air	**100**	**400**	**15, 16**
Li-ion	200	120	17, 18
Na-ion	280	100	19, 19
Na–S	380	200	20, 20
Pb-acid	490	40	20, 20
Ni–MH	1000	90	21, 21
Na–$NiCl_2$	1200	120	20, 20

† left reference number: cost; right reference number: specific energy

ESI Table 3 Survey of rechargeable areal capacity versus cycle life of Zn–air cells. We exclude literature values obtained using air-breathing electrodes containing scarce, high-risk elements, as defined by Fig. 1a. References are found in the main text.

Year	Cycle Life	Capacity (mA h cm_{geo}^{-2})	Reference
2016	15	20.0	38
2015	15	30.0	39
2020	**16**	**33.4**	**This work**
2018	24	2.08	40
2015	25	0.83	41
2017	32	10.0	42
2016	36	0.17	43
2016	100	0.83	44
2017	102	1.67	45
2020	120	0.21	46
2018	150	1.25	47
2015	160	1.00	48
2017	175	0.12	49
2017	180	0.83	50
2018	220	0.45	51
2016	270	4.00	52
2017	300	0.92	53
2019	600	0.46	54
2019	1000	0.84	55
2019	1000	1.67	56
2020	1100	1.67	57
2019	3600	2.08	58